Comparison of the heterogeneous photocatalysis of imidacloprid and thiacloprid – reaction mechanism, ecotoxicity, and the effect of matrices

Máté Náfrádi , Tamás Hlogyik, Luca Farkas, Tünde Alapi [*]

University of Szeged, Department of Inorganic and Analytical Chemistry, Dóm tér 7, H-6720 Szeged, Hungary

ABSTRACT

This comparative study is about the heterogeneous photocatalytic degradation of two neonicotinoids, namely imidacloprid and thiacloprid, focusing on the differences and similarities in their transformation and mineralization and the effect of various additives, matrices, and their inorganic components. Besides the dominant role of $^{\bullet}$OH, which was confirmed by the effect of pH and radical scavengers, the direct charge transfer may also contribute to the transformation, especially for imidacloprid; partly due to its enhanced interaction with the TiO$_2$ surface. There was a significant difference in the change of ecotoxicity, which decreased for thiacloprid but varied according to the maximum curve for imidacloprid, and interpreted by the effect of NO$_3^-$ formed. Dehalogenation and mineralization were fast and occurred in parallel with the neonicotinoid degradation; however, 20–25% organic carbon could not be removed, suggesting the formation of hardly oxidizable products. The fluorination of the TiO$_2$ has no significant effect on the transformation rates, but changed the product distribution, enhanced the dechlorination rate, and hindered the mineralization, confirming $^{\bullet}$OH-initiated formation of the hardly oxidizable intermediates. The negative effect of tap water and biologically treated domestic wastewater was significant. Although HCO$_3^-$ caused a slower transformation, the effect of matrices cannot be interpreted solely by the radical scavenging capacity of their organic and inorganic content.

1. Introduction

Industrial and agricultural activities result in the release of toxic, carcinogenic, endocrine-disrupting, or otherwise harmful chemicals, posing a serious threat to the environment, and possibly to human health. Special attention must be paid to neonicotinoid insecticides, which have caused serious ecological [1,2], environmental [3], and public health issues [4]. Imidacloprid (IMIDA), the first neonicotinoid produced in 1994 became one of the most widely used insecticides in the last decade [5]. IMIDA has the most serious environmental impact among neonicotinoids due to its negative effect on honeybees [6,7]. The European Union banned the open-field use of IMIDA due to its harmful effect on pollinators [8]. However, it is still extensively used worldwide, especially in the USA. Thiacloprid (THIA) is less toxic to bees than IMIDA but more dangerous to aquatic life forms. It also has an endocrine-disrupting effect [9]. The approval of THIA in the EU has also been withdrawn in 2020 based on the report of EFSA and the opposition of many EU Member States, while France has already banned its use since 2019 [10].

IMIDA has a relatively high solubility in water (610 mg dm^{-3}) [11], while THIA can be dissolved at a lower concentration (185 mg dm^{-3}) [12]. They are often used for seed treatment, but only a fraction of that (1.6–20%) is absorbed on the seeds; the rest remains in the soil [13] and can be detected even 10 months later [14]. The leaching of neonicotinoids from soils endangers the ecosystem and quality of ground and surface waters [1,13].

Application of Advanced Oxidation Processes (AOPs) offers a possible solution for removing neonicotinoids from water. These methods are based on the formation of highly reactive radicals, the most important of which is the hydroxyl radical ($^{\bullet}$OH). The rate constant of the reaction of THIA and IMIDA with different reactive species, such as $^{\bullet}$OH, hydrogen radical (H$\bullet$), and hydrated electron (e$_{aq}^-$) were determined by pulse radiolysis, while gamma radiolysis was applied for investigation of the reaction mechanism [15–17].

Many publications deal with the synthesis or modification of new materials suitable as photocatalysts [18–20]. Nevertheless, in terms of practical application, TiO$_2$ remained the most important photocatalysts. The commercially available TiO$_2$ is often used as a "reference" when the

efficiency of the photocatalysts is tested due to its high stability, non-toxicity, and photonic efficiency. The absorption of photons having higher energy than the bandgap (3.0 eV for rutile, and 3.2 eV for anatase [21]) results in the formation of an excited electron (e_{cb}^-) in the conduction band and a hole (h_{vb}^+) in the valence band of the TiO_2. The transformation of the organic compounds may undergo on the surface via direct charge transfer (with e_{cb}^- and h_{vb}^+) [22–24] or $^\bullet$OH-based reactions [25,26]. The surface-bound $^\bullet OH_{surf}$ ($\equiv$Ti–$^\bullet$OH) and 'free' $^\bullet OH_{bulk}$ in the aqueous bulk phase are often distinguished. The relative contribution of the reaction ways to the transformation depends on the chemical properties of the substrate, surface properties of the photocatalyst, the interaction between TiO_2 surface and substrate(s), and reaction conditions [25,27,28].

A simple way to change the TiO_2 surface properties is fluorination. The addition of F^- to aqueous TiO_2 suspensions results in the replacement of $\equiv$Ti-OH by $\equiv$Ti-F species and uniquely affects the surface properties, photocatalytic reactions, and photoelectrochemical behavior of TiO_2. Due to the fluorination, the change of valence band edge and conduction band edge facilitates the production of $^\bullet OH_{bulk}$ [29]. The much faster transformation of phenol for fluorinated than for bare TiO_2 was also reported and interpreted by that, the phenol degradation occurs almost exclusively via reaction with $^\bullet OH_{bulk}$ in the case of fluorinated TiO_2 opposite to the bare TiO_2 [30]. Moreover, the enhanced surface-bound $^\bullet$OH radical desorption by fluoride ions in the Helmholtz layers was proposed to enhance the $^\bullet OH_{bulk}$ concentration [31]. Accordingly, Ryu (2017) al. proved that fluorination enhanced the reaction between h_{vb}^+ and adsorbed H_2O, and the resulted ●OH can leave easily the surface [32]. At the same time, the production of $O_2^{\bullet-}/HO_2^\bullet$ was lower than that for pure TiO_2 because of the reduced interfacial electron transfer rate. Besides enhanced $^\bullet OH_{bulk}$ formation rate, the surface fluorination has other significant consequences due to the change of the surface functional groups, such as altering the Point of Zero Charge and Surface Charge of the photocatalyst, and the enhanced hydrophobicity of the TiO_2 surface, which change the adsorption properties [33]. The hindered adsorption can cause a decrease in the transformation rate, mainly when the substrate is adsorbed well on the surface of bare TiO_2 due to the interaction with the $\equiv$Ti-OH group [34–40]. Based on all these, the effect of fluorination of TiO_2 surface can give information about the kinetics and mechanism of photocatalytic degradation of substances.

For practical application, it is crucial how the matrix components affect efficiency. The effect is often attributed to the light filtration, reaction with reactive species [41–43], or the formation of TiO_2–organic matter complexes [44]. The effect of various inorganic anions (CO_3^{2-}, Cl^-, PO_4^{3-}, NO_3^-, SO_4^{2-}) was systematically investigated [45], and a decrease in $^\bullet$OH generation was observed for all anions. In some cases, however, a positive effect was observed. Although HCO_3^-/CO_3^{2-} are well-known $^\bullet$OH scavengers, the formation of carbonate radicals can enhance the photocatalytic degradation rate of some organic substances [46,47]. The effluents of wastewater treatment plants [42,48–50], synthetic wastewaters [48], pharmaceutical industry wastewater [41, 44], or river water [50,51] were used as a matrix in publications related to heterogeneous photocatalysis. The effect depends on the matrix, the model compound, and the interactions between the individual components and the TiO_2 surface [44]. The influence of the matrix and its components should not be underestimated in all aspects of photocatalytic degradation, and each matrix should be evaluated carefully. Degradation pathways can be promoted or inhibited, depending on the particular features of each system; our knowledge on this is still limited, even for TiO_2.

This study aims to investigate the heterogeneous photocatalytic transformation of IMIDA and THIA using commercial Aeroxide TiO_2 P25 photocatalyst and UV (300–400 nm) radiation. The work focuses on understanding the similarities and differences between the transformations of these neonicotinoids in the case of pure and fluorinated TiO_2. The effect of basic reaction parameters on the transformation rate,

mineralization rate, dehalogenation, and the formation of organic and inorganic products are also investigated and compared. The effect of reaction parameters, additives, and various radical scavengers was studied to provide information about the relative contribution of the direct charge transfer and $^\bullet$OH-based reactions to the transformation and mineralization. The change of ecotoxicity during photocatalytic treatment is followed by using an ecotoxicity test (*Vibrio fischeri* test organism). From the practical application point of view, the influence of matrices (tap water and biologically treated domestic wastewater) and their main inorganic components (Cl^- and HCO_3^-) on the efficiency are studied.

2. Experimental

2.1. Materials and methods

Analytical standards of IMIDA (>98%) and THIA (>99%) were provided by VWR and Sigma-Aldrich, respectively. Methanol (HiPerSolv CHROMANORM, super gradient grade for HPLC), tert-butanol (>99%), NaF (>99%), NaCl (>99%), 1,4-Benzoquinone (>98%), Oxalic acid (>99%), KI (>99%) and EDTA$\times$ 2Na (>99%) were provided by VWR. The high purity water was prepared using Milli-Q Integral Water Purification System (Merck Millipore). HCl (Sigma Aldrich, 99%) and NaOH (VWR, 99%) solutions were used to adjust the pH. TiO_2 Aeroxide P25 was purchased from Acros Organics. The tap water from Szeged (Hungary) and the biologically treated domestic wastewater were used as matrices. Their parameters are presented in Table S1.

In the case of each experiment, 250 cm^3 suspensions were irradiated in a cylindrical, temperature-controlled (T = 25 $\pm$ 0.5 °C) glass reactor and circulated (375 cm^3 min^{-1}) between the reactor and the reservoir by a peristaltic pump (Heidolph Pump drive 5001). The UV light source was a fluorescent lamp (GCL303T5/UVA, LightTech, dimensions: 307 mm $\times$ 20.5 mm, 15 W electric output) emitting in the 300–400 nm range with λ_{max} = 365 nm. Fig. S1 shows the experimental setup and photoreactor used. The photon-flux of the light source was measured using ferrioxalate actinometry [52] and found to be 5.57 $\times$ 10^{-6} mol_{photon} s^{-1}. The thickness of the irradiated suspension was 2.5 mm.

Before turning on the lamp, the suspension was saturated with air, O_2, N_2, or their mixture over 30 min (flow rates were controlled with a Cole-Palmer gas mixer). The concentration of dissolved O_2 was measured using a DO-40 dissolved O_2 meter (VWR). The photocatalytic experiments were started by turning on the light source. Before analysis, the samples were centrifuged and filtered (FilterBio PVDF-L, 0.22 μm) to remove the photocatalyst particles.

2.2. Analytical methods

The concentration of IMIDA and THIA was measured using an Agilent 1100 HPLC coupled with a diode array detector (DAD). The column (Lichrospher 100, RP-18; 5 μm) was thermostated at 25 °C, the flow rate of eluent (methanol:water = 55:45 (v/v) mixture) was 1.0 cm^3 min^{-1}, and 20 μL sample was injected. The detection was performed at 270 nm, 242 nm, and 210 nm. Under these conditions, IMIDA and THIA eluted at 3.58 and 7.10 min, respectively. During the determination of 6-chloronicotinic acid, the eluent was changed to a mixture of methanol and 0.10 v/v% formic acid (40:60 (v/v)), the retention time was 13.05 min

The transformation of IMIDA and THIA was characterized by the initial rate of transformation, obtained from linear regression fits to the concentration-time plot, up to 25% transformation. Some photocatalytic experiments were repeated three times to check the reproducibility of the experimental results. The accuracy of the initial transformation rates was within $\pm$ 7%.

The identification of intermediates was performed using an Agilent LC/MSD VL mass spectrometer coupled to the HPLC device. For HPLC-MS analysis, solid-phase extraction (SPE) was used as a sample pretreatment method. After conditioning (2.0 cm^3 water and 2.0 cm^3

methanol), a 50 cm^3 sample was loaded to the Phenomenex Stata-X 33 u cartridge. After washing (2.0 cm^3 water) and drying (10 min), elution was performed using 1.5 cm^3 methanol. The eluent was a mixture of water and methanol (30:70 (v/v)), and the flow rate was 0.75 cm^3 min^{-1}. The MS measurements were performed using APCI ion source and triple quadruple analyzer in positive mode (4000 V capillary voltage, 60 V fragmentor voltage, and 4.0 μA corona current). The flow rate of the drying gas was 4.0 dm^3 min^{-1}, and its temperature was 200 °C. The scanned mass range was between 50 and 500 AMU.

Spectrophotometric measurements were made with an Agilent 8423 UV-Vis spectrophotometer, using a 0.50 cm path-length cuvette. Total organic carbon (TOC) measurements were performed using an Analytik Jena N/C 3100 analyzer. The adsorbable organic halogen (AOX) content was measured with an Analytik Jena multi X 2500 analyzer. The sample volume was 15 cm^3, while the weight of the high purity activated carbon (adsorbent) was 100 mg. Sample pretreatment was performed using an APU-2 (Analytik Jena), with the column method. The chemical oxygen demand (LCK1414, 5.0–60.0 mg dm^{-3}), the concentration of nitrite (LCK342, 0.6–6.0 mg dm^{-3}), ammonium (LCK304, 0.015–2.0 mg dm^{-3}), and cyanide ion (LCK315, 0.01–0.6 mg dm^{-3}) was measured using colorimetric test kits (Hach Lange Ltd.) and a DR 2800 (Hach) Vis-spectrophotometer. The concentration of H$_2$O$_2$ (0.015–6.00 mg dm^{-3}) and nitrate ion (DMP method, 0.10–25.0 mg dm^{-3} NO$_3^-$−N) were determined by colorimetric test kits provided by Merck-Millipore, using a Spectroquant® Multy Vis-spectrophotometer.

Ecotoxicity tests (LCK480, Hach-Lange) based on the biolumines-cence measurements of marine bacteria *Vibrio fischeri* (*V. fischeri*) was applied to provide information on the acute toxicity of the multicom-ponent solution formed during photocatalysis·H$_2$O$_2$, formed during the transformation of organic substances, was decomposed in the samples by adding catalase enzyme (Sigma Aldrich, 2000–5000 unit mg^{-1}) before starting the ecotoxicity test. The enzyme concentration in the samples was adjusted to 0.20 mg dm^{-3}. The inhibition of biolumines-cence was measured using a Lumistox 300 (Hach Lange) luminometer after 15 min. The measurements were repeated three times to check the reproducibility.

3. Results and discussion

3.1. Effect of dissolved O$_2$, TiO$_2$, and neonicotinoid concentration

At constant dissolved O$_2$, and substrate concentrations, the reaction rate is determined by the number of photogenerated charges, which can be increased with TiO$_2$ dosage and is limited by the photon flux. In this work, the optimum TiO$_2$ dosage was 0.5 g dm^{-3} for THIA and 1.0 g dm^{-3} for IMIDA. The transformation of THIA was negligible (9 ×10^{-9} felM s^{-1}) without TiO$_2$, but IMIDA slowly transformed (2.8 ×10^{-8} M s^{-1}) (Fig S2a) due to the overlap of its absorption spectra with the emission spectra of the light source (Fig. S3). For further experiments, a con-centration of 1.0 g dm^{-3} TiO$_2$ was used to provide the complete ab-sorption of UV light by TiO$_2$ and exclude the direct photolysis of neonicotinoids. Both IMIDA and THIA (1.0 ×10^{-4} M) adsorbed poorly (<2%) in the range of 0.25–1.50 g dm^{-3} TiO$_2$ dosage.

The efficient e$_{cb}^-$ capture, such as dissolved O$_2$, plays a crucial role in heterogeneous photocatalysis. In O$_2$-free 1.0 g dm^{-3} TiO$_2$ containing suspension, a slow transformation of IMIDA (2.84 ×10^{-8} M s^{-1}) was observed, while THIA transformation was negligible (<5 ×10^{-9} M s^{-1}) (Fig S2b). Since both neonicotinoids react fast with •OH (k$_{IMIDA+•OH}$ = 6.97 ×10^9 M^{-1} s^{-1} [17]; k$_{THIA+•OH}$ = 4.80 ×10^9 M^{-1} s^{-1} [16]) and e$^-_{aq}$ (k$_{IMIDA+eaq-}$ = 5.10 ×10^9 M^{-1} s^{-1} [17]; k$_{THIA+eaq-}$ = 1.0 ×10^{10} M^{-1} s^{-1} [16]); the role of e$_{cb}^-$ capture may be partially taken over by IMIDA in O$_2$-free suspension, and the direct charge transfer can be responsible for its slow transformation. Besides the reaction with the e$_{cb}^-$, O$_2$ has an essential role in the formation of •OH from O$_2^{•-}$ [53], and opening new pathways for the transformation of carbon-centered radicals via organic peroxyl radicals [54]. Even 5% (v/v) O$_2$ content in O$_2$/N$_2$ mixture has

dramatically increased the transformation rate; its further increase has no significant effect; thus, experiments were performed in air-saturated suspensions (c$_{O2}$ = 1.75 ×10^{-4} M).

The effect of the initial substrate concentration on the transformation rate is described by pseudo-first-order kinetics, which is rationalized in terms of the Langmuir-Hinshelwood (L-H) model (Fig. 1). The linearized form applied is the following:

$$\frac{1}{r_0} = \frac{1}{K \times k \times c_{eq}} + \frac{1}{k} \tag{1}$$

where r$_0$ is the initial transformation rate, c$_{eq}$ is the equilibrium con-centration of the substrate, *K* represents the equilibrium constant for adsorption onto the semiconductor surface, and *k* reflects the limiting rate constant at maximum coverage under the given experimental con-ditions. The k and K values were 3.71 × 10^{-7} M s^{-1} and 7.23 × 10^3 s^{-1} for IMIDA, and 2.22 × 10^{-7} M s^{-1} and 2.85 × 10^4 s^{-1} for THIA (Fig. 1), respectively. The higher *K* value of IMIDA suggests a pronounced interaction with the surface compared to THIA.

At 1.0 g dm^{-3} TiO$_2$ dosage, the apparent quantum yields of the transformation were 0.0106(± 0.0018) for IMIDA, while a slightly lower value of 0.0092(± 0.0014) was determined for THIA (c$_0$ > 1.4 ×10^{-4} M).

3.2. Formation of organic and inorganic products

UV-Vis absorption spectrum of the IMIDA and THIA has a maximum at 270 and 242 nm, respectively. The absorbance at 270 and 242 nm decreased more slowly than the concentration of IMIDA or THIA (Fig. S4), suggesting the formation of intermediates containing 2-chlor-opyridine moiety. The maximum of the spectra did not shift during the treatment (Fig. S5.) indicating that 2-chloropyridine moiety remains unchanged during the first steps. There was no significant shift, new peaks, or shoulders on the longer wavelength side of the main peak, suggesting that the hydroxylation of the 2-chloropyridine moiety of the target substances is not significant.

HPLC/MS measurements (Table S2) were performed to identify the aromatic products. For IMIDA, the •OH mainly attacks the imidazole ring, nitramide group, and −CH$_2$ − group (the "bridge" between the rings); the reaction with the 2-chloropyridine ring is less favored [15–17,55]. The reaction of •OH with the imidazole ring results in hy-droxylated (Im1, Im2, Im3, and Im5, Im6) products (Fig. 2). Carbon-centered radicals formed due to the reaction of •OH with −CH$_2$ − group can result in an amide (Im4) or cause bond cleavage and the formation of 6-chloronicotinic acid (Im7). The nitrogen content of IMIDA was converted to NO$_3^-$ and NH$_4^+$, their concentration ratio is close to 1:1 (Fig. 5e, 5 f). NO$_2^-$ was also detected at low concentrations.
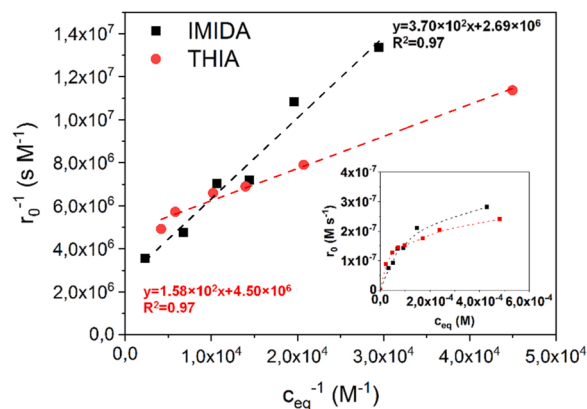

Fig. 1. The linear fits according to the Langmuir-Hinshelwood model and the initial transformation rates of IMIDA and THIA versus the equilibrium con-centration (inserted figure).
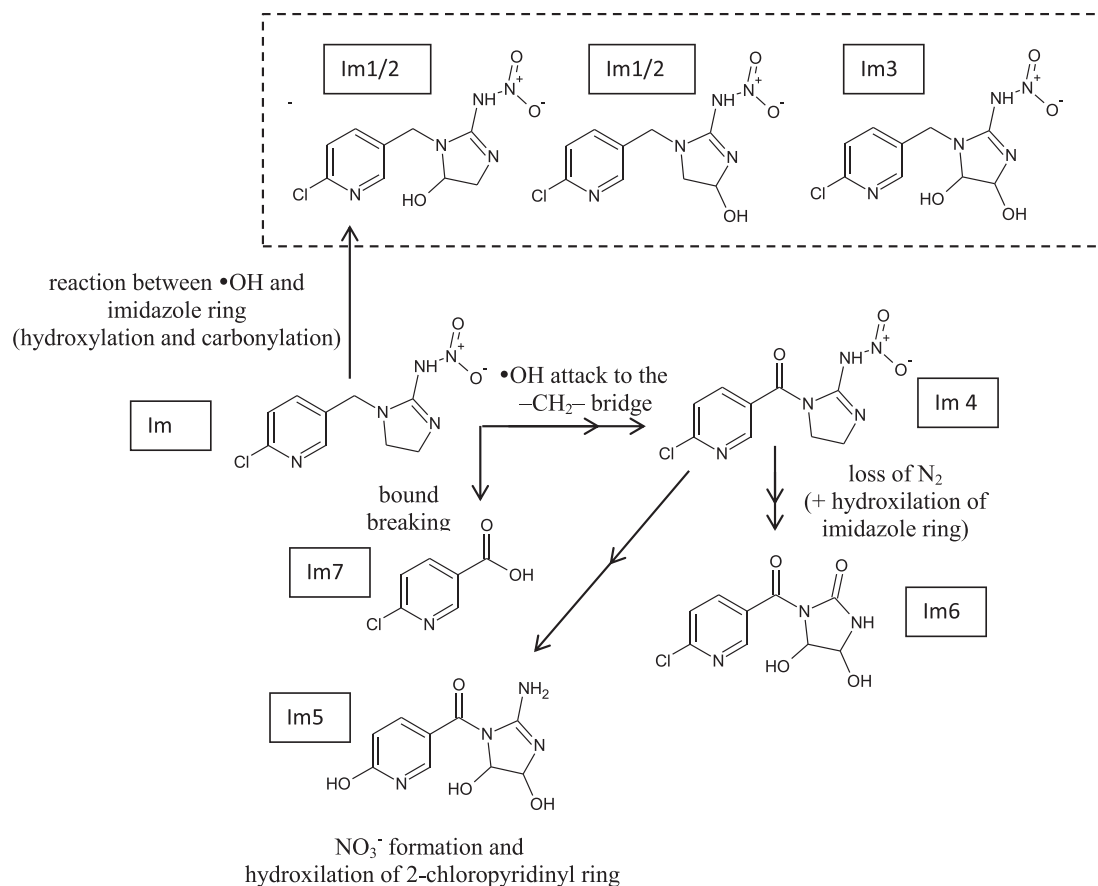
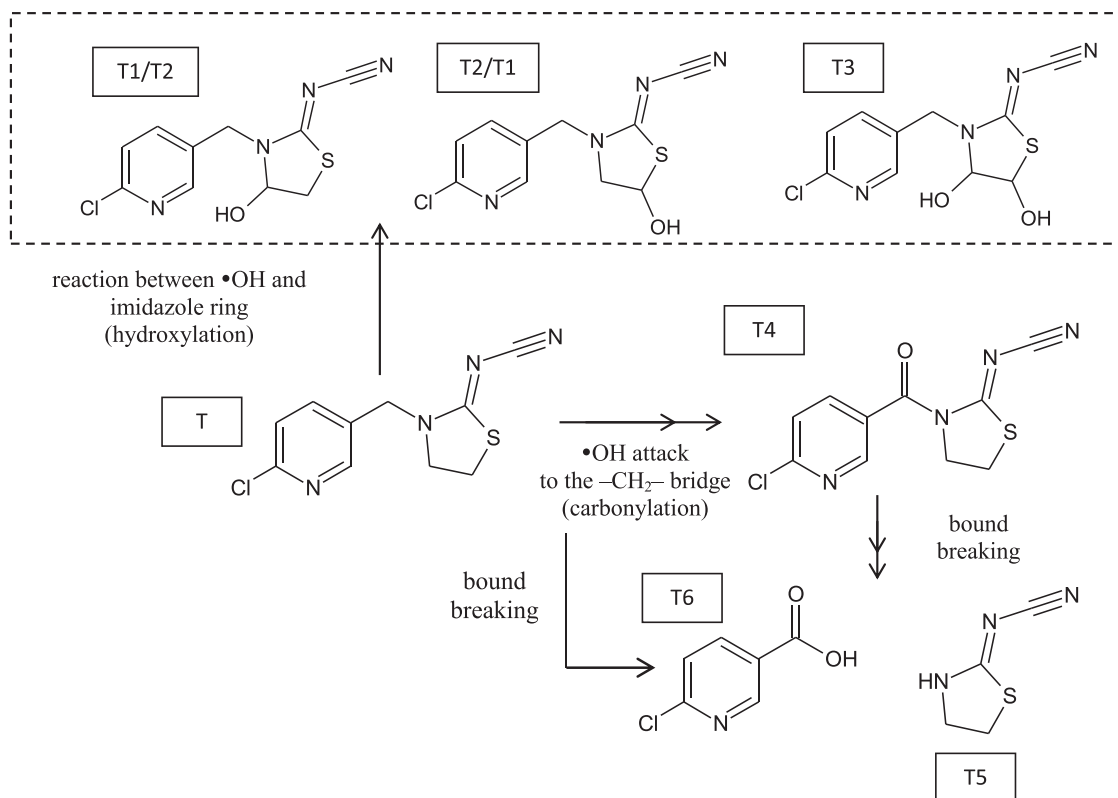**Fig. 2.** The products of IMIDA detected by HPLC-APCI-MS in positive mode.

Fig. 3. The products of THIA detected by HPLC-APCI-MS in positive mode.

Calza et al. reported NO_3^- formation from nitro-group and NH_4^+ formation from amino groups; the mineralization of N-containing aromatic rings can result in both inorganic ions [51]. The NO_3^- formation is likely to be associated with the formation of Im5. The transformation of the nitramide group can be partly accompanied by N_2 [15] formation.

The T1, T2, T3 products of THIA form via hydroxylation of the thiazolidine ring (Fig. 3). Similar to IMIDA, the reaction between $-CH_2$ $-$ bridge and $^\bullet OH$ can result in a carbonylated product (T4), or bond-breaking (T5 and T6) [55]. The mineralization of THIA resulted in NH_4^+ (Fig. 5e), NO_3^- was not detected in this case, confirming that NO_3^- formation mainly relates to converting the nitro group and NH_4^+ forms from N-containing aromatic rings.

3.3. The effect of additives

The effect of various additives (radical scavengers, poorly or well-adsorbed organic matter, and inorganic ions) can provide information about the relative contribution of the reactive species to the transformation. These additives also shed light on how the matrix components may affect heterogeneous photocatalysis efficiency in "real water" which contains many different organic and inorganic components. Due to the complexity of a heterogeneous system, an additive can change several parameters [25,56–59] therefore, evaluation of results should be done with care. The effect of additives was compared based on Relative Scavenging Capacity (RSC) values. The RSC was calculated according to the following equation:

$$RSC = \frac{c_{scav} \times k_{scav}}{(c_n \times k_n + c_{scav} \times k_{scav})}$$

where c_n and c_{scav} is the initial concentration of neonicotinoid (1.0×10^4 M) and additive, and k_n and k_{scav} are the reaction rate constants of neonicotinoid and additive with $^\bullet OH$ (Table S3).

The negative effect of tert-Butanol ($k_{(t-BuOH+^\bullet OH)} = 6.0 \times 10^8$ M^{-1} s^{-1}) demonstrates the role of $^\bullet OH$ (Fig. 4.) The decrease in the transformation rate corresponds to the RSC value. Another poorly-adsorbed organic additive was 1,4-benzoquinone (1,4-BQ), which reacts with $^\bullet OH$ (1.2×10^9 M^{-1} s^{-1}), with $O_2^{\bullet -}$ (9.0×10^8 M^{-1} s^{-1} [60]) and also with photogenerated e_{cb}^- ($k(1,4-BQ+e_{aq}^-) = 2.3 \times 10^{10}$ M^{-1} s^{-1}) [61, 62], even in the presence of dissolved O_2. The decrease of transformation rate is more pronounced than expected according to the RSC value, suggesting that reaction with e_{cb}^- can contribute to the conversion of neonicotinoids. Another reason can be the inhibition of $O_2^{\bullet -}$ formation, which can also be a $^\bullet OH$ source. Iodide ion was used as a $^\bullet OH_{bulk}$ scavenger (1.1×10^{10} M^{-1} s^{-1}), but it reacts with h_{vb}^+ too. In the case of IMIDA, the negative effect of I^- is more pronounced than t-BuOH, especially at lower scavenging capacity values (Fig. 4),

suggesting the relative contribution of h_{vb}^+. The slow transformation of IMIDA under O_2-free conditions can be due to its simultaneous reactions with both photogenerated charges.

The $EDTA^{2-}$ is a well adsorbed organic substance and reacts with both $^\bullet OH$ (4.0×10^8 M^{-1} s^{-1}) and h_{vb}^+ [63]. The $EDTA^{2-}$ decreased the transformation rates significantly even at 1:1 concentration ratios, although no more than 5% of $^\bullet OH$ is scavenged (RSC values are 0.05 and 0.01). Higher $EDTA^{2-}$ concentration completely inhibited the transformation of neonicotinoids due to the combined effect of the strong interaction with the TiO_2 surface and its reaction with $^\bullet OH$. This effect is less significant for THIA than for IMIDA, which can be explained by a stronger interaction between the TiO_2 surface and IMIDA.

Comparing the effect of various scavengers and additives, we can state that the dominant reactive species is the $^\bullet OH$ in the transformation of both neonicotinoids. The effect of 1,4-BQ, and I^-, the relatively high rate constants of neonicotinoids toward e_{aq}^-, and the slow transformation of IMIDA in O_2-free suspension suggest the contribution of direct charge transfer to the transformation.

3.4. Dehalogenation and mineralization

The Cl-containing aromatic substances are often toxic or otherwise harmful xenobiotics in the environment. Thus the dechlorination is an essential process for their disposal. In both cases, most of the detected aromatic products contain $-Cl$ moiety; however, the AOX measurement (Fig. 5d) proves that dehalogenation occurs parallel with IMIDA or THIA transformation. Consequently, the dechlorination is probably due to further transformation of the hydroxylated or carbonylated products. The hydroxylated products demonstrated the importance of $^\bullet OH$ in the photocatalytic transformation of both IMIDA and THIA, but the possibility of direct charge transfer cannot be excluded this way. Theurich et al. [64] interpreted the dechlorination of 4-chlorophenol due to the direct charge transfer reaction, and dehalogenation was proposed via a one-electron reduction mechanism in the case of gamma radiolysis of THIA [16].

One advantage of heterogeneous photocatalysis is the simultaneous transformation of the target compound and its intermediates due to the low selectivity of $^\bullet OH$. During 30 min treatment, the neonicotinoids were converted, and the total organic carbon concentration (TOC) decreased linearly by half and then significantly slowed down. No further changes were observed after 90 min of treatment, and finally, 20% of the remaining TOC could not be removed. (Fig. 5c). Similar to the TOC value, there is no change of NH_4^+ concentration after 90 min, but NO_3^- increases slowly. A similar trend of TOC was reported for the pesticide atrazine because of the formation of very stable cyanuric acid [65,66]. Our observations suggest stable products of neonicotinoids,
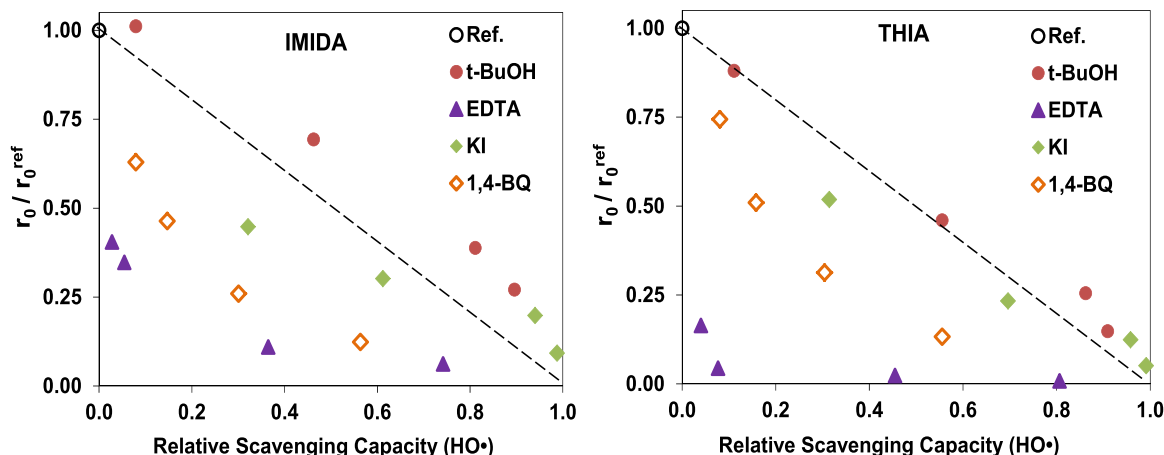

Fig. 4. Relative transformation rates of IMIDA and THIA in the presence of various additives versus the relative $^\bullet OH$ scavenging capacity (RSC values).
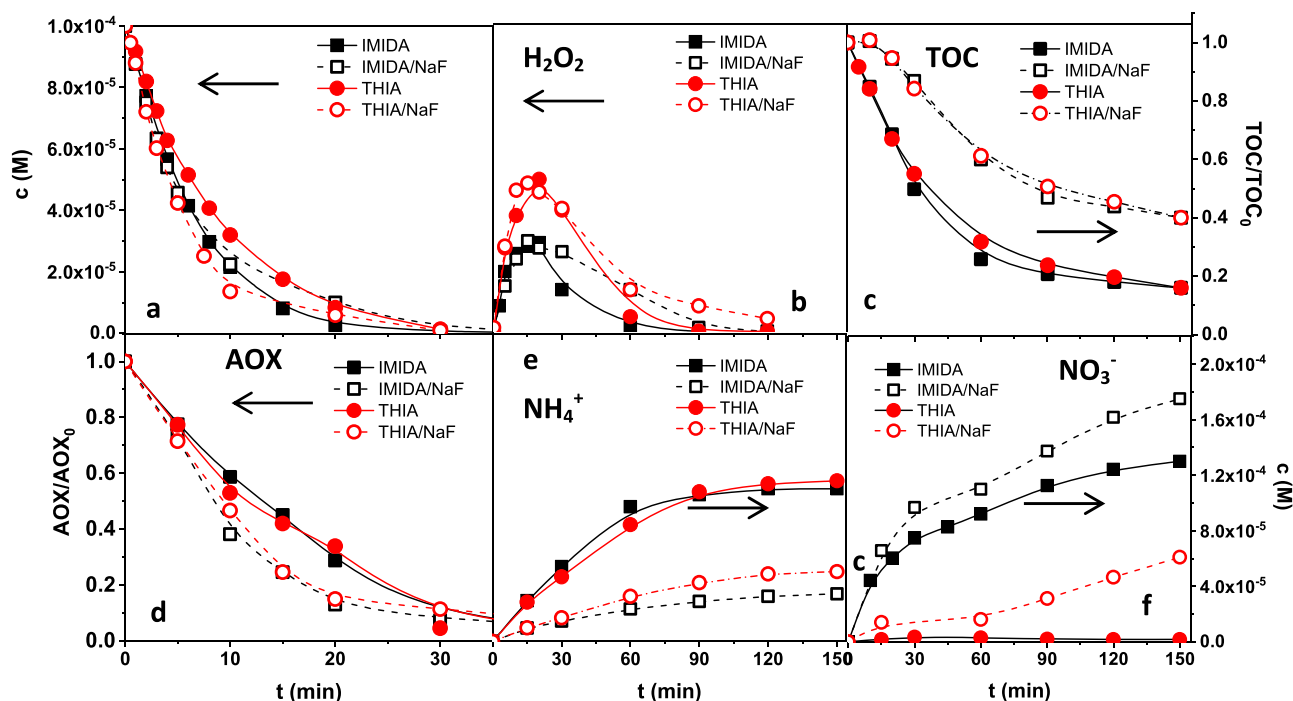
Fig. 5. The concentration of neonicotinoids (a), H_2O_2 (b), relative TOC (c) and AOX (d) concentration, and the concentration of NH_4^+ (e) and NO_3^- (f) in treated suspensions without and with the addition of NaF.

which are resistant to further oxidation and just slowly transformed. Some authors also reported a high mineralization efficiency initially [55], but hardly oxidizable products were not reported.

The formation of H_2O_2 accompanies the conversion of organic compounds due to the recombination of $HO_2^\bullet$ and $O_2^{\bullet-}$ (1.02×10^8 M^{-1} s^{-1} [67]), which are formed during the transformation of organic peroxyl radicals [54]. The H_2O_2 concentration increases fast and reaches the maximum value (which is two times higher for THIA than for IMIDA) when the neonicotinoid is wholly degraded, and there is no H_2O_2 after 90 min, although the solution still contains 20% of the initial TOC (Fig. 5b).

3.5. Effect of fluorination

The addition of NaF (5.0×10^3 M) to an aqueous suspension of TiO_2 (1.0 g L^{-1}) fluorinates its surface by replacing the terminal $\equiv$Ti–OH groups with $\equiv$Ti–F groups [37]. The $\equiv$Ti–F groups enhance the separation of photogenerated charges and the formation of "free" $^\bullet OH_{bulk}$ [30,34–36] but reduce the interfacial electron transfer rates by holding trapped electrons [31,36,39,68]. The increased conversion rate of many organic compounds has been interpreted as the consequence of higher $^\bullet OH_{bulk}$ concentration [30,34–38]. Besides all of these, the importance and contribution of direct charge transfer to the transformation can also change [38–40,68,69]. The overall effect of fluorination can significantly depend on the change of surface adsorption properties, but in the case of IMIDA and THIA, fluorination does not affect the adsorbed amount.

In the case of fluorinated TiO_2, t-BuOH reduces the conversion rate to a slightly greater extent, confirming the enhanced contribution of $^\bullet OH$-initiated reactions comparing to pure TiO_2. However, the effect of 1,4-BQ is less significant because of the inhibition of the charge transfer reactions (Fig S7).

The addition of NaF did not affect the transformation rate of IMIDA but enhanced that of THIA (Fig. 5a). The change in the distribution of IMIDA intermediates (an increase of the concentration of Im3 containing two hydroxyl groups) suggests that the relative contribution of $^\bullet OH$ and charge transfer initiated processes to IMIDA conversion differs for TiO_2

and fluorinated TiO_2. For THIA, the enhanced $^\bullet OH$ concentration is probably the dominant effect because of the weaker interaction with the TiO_2 surface; consequently, there was no significant change in the aromatic product distribution (Fig. S6).

The enhanced dechlorination, the greatly hindered mineralization, and the change of the concentration of N-containing inorganic ions underline the change in the transformation mechanism (Figs. 5c, 5d) of neonicotinoids and/or their products. The NH_4^+ concentration was reduced by half (THIA) and a third (IMIDA), while NO_3^- concentration increased (Figs. 5e, 5 f). These all support the fact that the conversion of the neonicotinoids (especially of IMIDA) and their intermediates involve the direct charge transfer beside the $^\bullet OH$-based reactions and the formation of hardly oxidizable intermediate(s) is likely to occur in $^\bullet OH$-initiated reactions.

3.6. Ecotoxicity assay

The change of toxicity during treatment is an important aspect to evaluate the efficacy. The publications about neonicotinoids reported increased [15] and decreased toxicity [55,70,71]. The impact of formed H_2O_2 is often neglected; however, H_2O_2 is also toxic [72], and its accumulation occurs in the case of the oxidative transformation of organic substances. In this work, H_2O_2 was eliminated from the samples by catalase enzyme addition.

The ecotoxicity test is based on the inhibition of bioluminescence (%) emitted by *Vibrio fischeri* bacteria. The toxicity of THIA solutions was reduced from 49% to 20% inhibition over 30 min treatment (Fig. 6), contrary to the observation of Berberidou et al. [55], who reported the change according to the maximum curve. During 30 min, THIA decomposed, and the TOC value decreased by half (Fig. 5c). In the first 30 min of the treatment of IMIDA solution, the toxicity enhanced just slightly (Fig. 6). After 30 min the IMIDA and most of its aromatic intermediates are already converted, the solution no longer contains Cl-containing organic matter, and the TOC decreased by half, similar to THIA. The maximum value of the inhibitory effect (60 min) coincides with the onset of slowing of the TOC change and the reaching/approaching the maximum NH_4^+ and NO_3^- concentration.
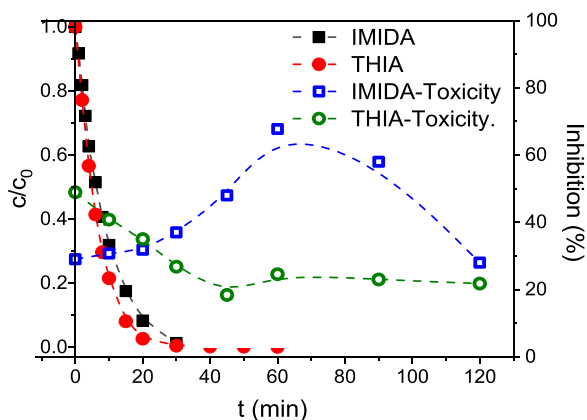
Fig. 6. The concentration of IMIDA and THIA, and the inhibition of bioluminescence as a function of the time of treatment.

Dell'Arciprete [15] also reported the formation of toxic products from IMIDA while Kitsiou [71] described the reduced toxicity.

The NO_3^-, detected only for IMIDA, is nontoxic to *Vibrio fischeri*, but under UV (300–400 nm) radiation can transform into highly toxic NO_2^- [73,74], which reacts fast with $^\bullet OH$ (6.0×10^9 M^{-1} s^{-1}) [75]. The photochemical circulation between NO_3^- and NO_2^- in an aqueous solution under UV radiation is a very complex process [73], especially in the presence of TiO_2. The sensitivity of *Vibrio Fischeri* to NO_2^- [74] was checked with 1.0×10^{-4} M $NaNO_2$ solution, but a significant effect was not observed. Accordingly, the increase in ecotoxicity is likely due to intermediates or their combined effects with NO_2^-.

3.7. The effect of pH, inorganic ions, and matrices

The pH dependence of the transformation rates was measured in a suspension having constant ionic strength (5.0×10^{-3} M NaCl). The added NaCl did not affect the transformation rates (Fig. 7a). The pH was adjusted with HCl or NaOH solutions. Between pH 3.0 and 9.0 there is no change of the protonation state of neonicotinoids, but the $\equiv$Ti–OH groups of TiO_2 can undergo protonation and deprotonation processes [40]. The decrease of pH from 6.5 (the point of zero charge of Aeroxid P25 is 6.3–6.6) changed the surface charge into positive and reduced the transformation rate significantly (Fig. 7a), probably due to the thermodynamically unfavorable formation of $^\bullet OH$ under acidic conditions. The increase of pH from 6.5 to 9.0 had no effect.

The pH of the suspension was 6.3 when Milli-Q water was used and increased to 8.6 when HCO_3^- was added, or tap water (7.9) and BTD

wastewater (8.2) was used as matrix. Within this range, the pH effect on the transformation rate is negligible (Fig. 7a), and the surface charge is neutral or negative. Even the tap water, having a low COD value (4.2 mg dm^{-3}), and high ionic (Cl^- (8.75 mg dm^{-3}) and HCO_3^- (373 mg dm^{-3})) content (Table S1), significantly decreased the efficiency (Fig. 7b). The COD value of the biologically treated domestic wastewater (BTD ww) (24 mg dm^{-3}) is similar to the COD value of 1.0×10^{-4} M THIA (29 mg dm^{-3}) or IMIDA (21 mg dm^{-3}) solution, and Cl^- (120 mg dm^{-3}) and HCO_3^- (525 mg dm^{-3}) concentration is even higher than that of tap water. Thus, organic content should also contribute significantly to the adverse effect via competition for $^\bullet OH$ and cause a more significant negative impact.

The effect of 120 mg dm^{-3} Cl^- and 525 mg dm^{-3} HCO_3^- (the concentrations measured in BTD wastewater) in MilliQ water separately and simultaneously (Fig. 7b) was examined. The effect of Cl^- was negligible, probably because of its dual effect, which can be attributed to its ability to convert $^\bullet OH$ ($k_{(^\bullet OH + Cl)} = 3.0 \times 10^9$ M^{-1} s^{-1} [76]) to reactive and selective radicals ($Cl^\bullet$, $Cl_2^{\bullet-}$, $ClOH^{\bullet-}$), but $^\bullet OH$ regeneration is also possible [77]. The addition of HCO_3^- reduced the conversion rate by 30% and 39% for THIA and IMIDA, respectively, although no more than 10% of $^\bullet OH$ reacts with HCO_3^- (1.0×10^7 M^{-1} s^{-1} [78]). HCO_3^- may also react with h_{vb}^+ [79,80], and generate carbonate radical anions ($CO_3^{\bullet-}$). The reaction with h_{vb}^+ may contribute to the inhibition effect, since the $CO_3^{\bullet-}$ is moderately reactive towards neonicotinoids ($k_{(IMIDA + CO_3\bullet-)} = 4.0 \times 10^6$ M^{-1} s^{-1}; $k_{(THIA + CO_3\bullet-)} = 1.5 \times 10^5$ M^{-1} s^{-1} [81]). Moreover, the HCO_3^- caused visibly increased aggregation of TiO_2 particles, which could contribute to the reduced efficiency. The effect of both ions cannot be interpreted solely by their reactions with $^\bullet OH$. The effect of Cl^- and HCO_3^- mixture was similar to that of HCO_3^-, but was significantly less than tap water or BTD wastewater (Fig. 7b). The fluorination could not protect the surface of TiO_2 against the effect of HCO_3^-, moreover, the negative effect was even more pronounced in the presence of fluoride. Also, there was no significant difference between the transformation rates determined for fluorinated and pure TiO_2 in the matrices. The treatment time required to convert 90% of the neonicotinoid (1.0×10^{-4} M) was doubled (20 → 45 min for IMIDA and 20 → 55 min for THIA) in the tap water, and more than tripled (20 → 60 min for IMIDA and 20 → 90 min for THIA) in biologically treated domestic water, which can multiply the electrical energy required to operate the light sources, and consequently, the cost of this method.

4. Conclusions

A detailed investigation of the heterogeneous photocatalysis of two neonicotinoids, namely IMIDA and THIA is presented. The interaction
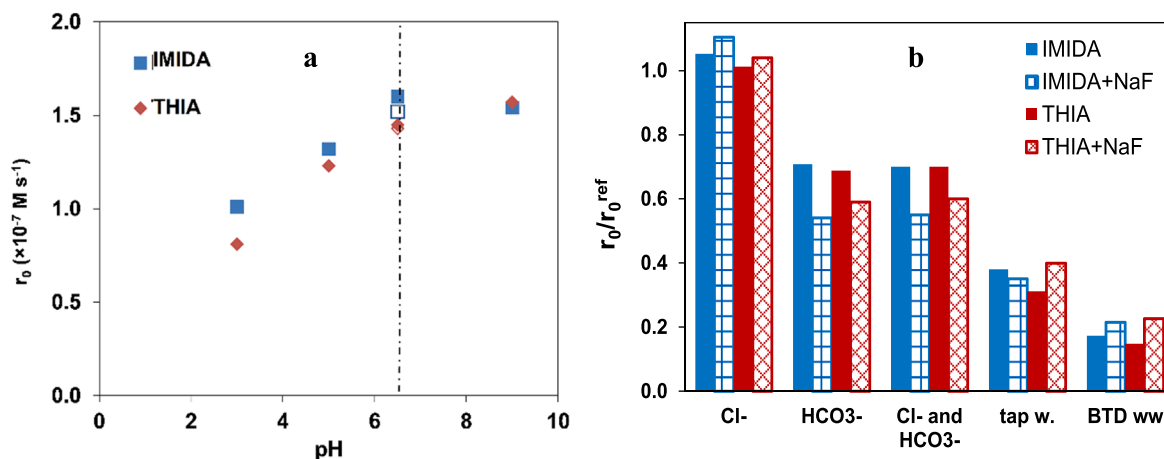

Fig. 7. Effect of pH (a) (empty symbols show the r_0 determined without NaCl addition, full symbols show data determined at constant ionic strength ($c_{NaCl} = 5.0 \times 10^{-3}$ M)) and the effect of matrices and inorganic matrix components (b).

between the neonicotinoids and TiO_2 surface, the formation of organic and inorganic products, the effect of various additives, fluorination, and matrices (tap water and biologically treated domestic wastewater) were investigated. The conclusions can be summarized as follows:

i. For both neonicotinoids, the $^\bullet$OH-initiated transformation is decisive, but the direct charge transfer also plays a role, especially in the case of IMIDA due to its enhanced interaction with TiO_2 surface.

ii. When examining the effect of radical scavengers, the results should be evaluated considering the interaction between the surface of photocatalyst, neonicotinoids, and additives.

iii. Although fluorination increased the rate of $^\bullet$OH formation, it slightly affected the transformation rate of neonicotinoids. Changes in the rate of formation of organic and inorganic products (NH_4^+ and NO_3^-) and the rate of dehalogenation and mineralization clearly indicated the change in the contribution of $^\bullet$OH-initiated reactions and direct charge transfer. All this points out that changes in the transformation rate of the target substance alone are not sufficient to draw appropriate conclusions, and detailed studies are needed.

iv. In contrast to the similar transformation and mineralization rate of THIA and IMIDA, the time dependence of the toxicity was different; that decreased for THIA and increased for IMIDA, which can be attributed to the combined effect of toxic organic intermediates and NO_3^-/NO_2^- formation.

v. The reduced efficiency in matrices is due to the combination of several factors: the high ionic content, which enhances the aggregation of TiO_2 particles, the $^\bullet$OH scavenging effect of HCO_3^- and organic substances, and change of the surface properties of the TiO_2 particles.

Funding

CRediT authorship contribution statement

Tünde Alapi: Conceptualization, Writing - Original Draft, Writing-Reviewing and Editing, Supervision, Funding acquisition **Máté Náfrádi:** Conducting a research and investigation process, specifically performing the experiments, or data/evidence collection, Writing - Original Draft, Writing- Reviewing and Editing **Tamás Hlogyik:** performing the experiments, or data/evidence collection **Luca Farkas:** performing the experiments, or data/evidence collection.

Conflicts of interest

The authors declare that they have no known competing financial interests or personal relationships that could have influenced the work reported in this paper.

Declaration of Competing Interest

The authors declare that they have no known competing financial interests or personal relationships that could have appeared to influence the work reported in this paper.

Appendix A. Supporting information

Supplementary data associated with this article can be found in the online version at doi:10.1016/j.jece.2021.106684.

References

[1] C.A. Morrissey, P. Mineau, J.H. Devries, F. Sanchez-Bayo, M. Liess, M.C. Cavallaro, K. Liber, Neonicotinoid contamination of global surface waters and associated risk to aquatic invertebrates: a review, Environ. Int. 74 (2015) 291–303, https://doi.org/10.1016/j.envint.2014.10.024.

[2] EFSA report, Guidance on the risk assessment of plant protection products on bees (Apis mellifera, Bombus spp. and solitary bees), EFSA J. 11 (2013), https://doi.org/10.2903/j.efsa.2013.3295.

[3] J.M. Bonmatin, C. Giorio, V. Girolami, D. Goulson, D.P. Kreutzweiser, C. Krupke, M. Liess, E. Long, M. Marzaro, E.A. Mitchell, D.A. Noome, N. Simon-Delso, A. Tapparo, Environmental fate and exposure; neonicotinoids and fipronil, Environ. Sci. Pollut. Res. 22 (2015) 35–67, https://doi.org/10.1007/s11356-014-3332-7.

[4] W. Han, Y. Tian, X. Shen, Human exposure to neonicotinoid insecticides and the evaluation of their potential toxicity: an overview, Chemosphere 192 (2018) 59–65, https://doi.org/10.1016/j.chemosphere.2017.10.149.

[5] P. Jeschke, R. Nauen, M. Schindler, A. Elbert, Overview of the status and global strategy for neonicotinoids, J. Agric. Food Chem. 59 (2011) 2897–2908, https://doi.org/10.1021/jf101303g.

[6] A.N. Arce, A.R. Rodrigues, J. Yu, T.J. Colgan, Y. Wurm, R.J. Gill, Foraging bumblebees acquire a preference for neonicotinoid-treated food with prolonged exposure, Proc. R. Soc. B Biol. Sci. 285 (2018). https://doi.org/10.1098/rspb.2018.0655.

[7] L. Tison, M.L. Hahn, S. Holtz, A. Rößner, U. Greggers, G. Bischoff, R. Menzel, Honey bees' behavior is impaired by chronic exposure to the neonicotinoid thiacloprid in the field, Environ. Sci. Technol. 50 (2016) 7218–7227, https://doi.org/10.1021/acs.est.6b02658.

[8] Document:32018R0783, , Commission Implementing Regulation (EU) 2018/783 of 29 May 2018 admening implementing regulation (EU= No 540/2011 as regards the condtions of approval of the active substance imidacloprid, . J. Eur. Union. (2018) 2016–2019.

[9] E. Caron-Beaudoin, R. Viau, A.A. Hudon-Thibeault, C. Vaillancourt, J.T. Sanderson, The use of a unique co-culture model of fetoplacental steroidogenesis as a screening tool for endocrine disruptors: The effects of neonicotinoids on aromatase activity and hormone production, Toxicol. Appl. Pharmacol. 332 (2017) 15–24, https://doi.org/10.1016/j.taap.2017.07.018.

[10] H. Abdourahime, M. Anastassiadou, M. Arena, D. Auteri, S. Barmaz, A. Brancato, D. Brocca, L. Bura, L. Carrasco Cabrera, A. Chiusolo, C. Civitella, D. Court Marques, F. Crivellente, L. Ctverackova, C. De Lentdecker, M. Egsmose, G. Fait, L. Ferreira, V. Gatto, L. Greco, A. Ippolito, F. Istace, S. Jarrah, D. Kardassi, R. Leuschner, A. Lostia, C. Lythgo, J.O. Magrans, P. Medina, S. Messinetti, D. Mineo, I. Miron, S. Nave, T. Molnar, L. Padovani, J.M. Parra Morte, R. Pedersen, M. Raczyk, H. Reich, S. Ruocco, K.E. Saari, A. Sacchi, M. Santos, R. Serafimova, R. Sharp, A. Stanek, F. Streissl, J. Sturma, C. Szentes, J. Tarazona, A. Terron, A. Theobald, B. Vagenende, P. Vainovska, J. Van Dijk, A. Verani, L. Villamar-Bouza, Peer review of the pesticide risk assessment of the active substance thiacloprid, EFSA J. 17 (2019), https://doi.org/10.2903/j.efsa.2019.5595.

[11] F. Flores-Céspedes, C.I. Figueredo-Flores, I. Daza-Fernández, F. Vidal-Peña, M. Villafranca-Sánchez, M. Fernández-Pérez, Preparation and characterization of imidacloprid lignin-polyethylene glycol matrices coated with ethylcellulose, J. Agric. Food Chem. 60 (2012) 1042–1051, https://doi.org/10.1021/jf2037483.

[12] M.A. Beketov, M. Liess, Acute and delayed effects of the neonicotinoid insecticide thiacloprid on seven freshwater arthropods, Environ. Toxicol. Chem. 27 (2008) 461–470, https://doi.org/10.1897/07-322R.1.

[13] T.J. Wood, D. Goulson, The environmental risks of neonicotinoid pesticides: a review of the evidence post 2013, Environ. Sci. Pollut. Res. 24 (2017) 17285–17325, https://doi.org/10.1007/s11356-017-9240-x.

[14] C. Botías, A. David, J. Horwood, A. Abdul-Sada, E. Nicholls, E. Hill, D. Goulson, Neonicotinoid residues in wildflowers, a potential route of chronic exposure for bees, Environ. Sci. Technol. 49 (2015) 12731–12740, https://doi.org/10.1021/acs.est.5b03459.

[15] M.L. Dell'Arciprete, L. Santos-Juanes, A.A. Sanz, R. Vicente, A.M. Amat, J.P. Furlong, D.O. Mártire, M.C. Gonzalez, Reactivity of hydroxyl radicals with neonicotinoid insecticides: Mechanism and changes in toxicity, Photochem. Photobiol. Sci. 8 (2009) 1016–1023, https://doi.org/10.1039/b900960d.

[16] G. Rózsa, L. Szabó, K. Schrantz, E. Takács, L. Wojnárovits, Mechanistic study on thiacloprid transformation: Free radical reactions, J. Photochem. Photobiol. A Chem. 343 (2017) 17–25, https://doi.org/10.1016/j.jphotochem.2017.04.012.

[17] G. Rózsa, M. Náfrádi, T. Alapi, K. Schrantz, L. Szabó, L. Wojnárovits, E. Takács, A. Tungler, Photocatalytic, photolytic and radiolytic elimination of imidacloprid from aqueous solution: Reaction mechanism, efficiency and economic considerations, Appl. Catal. B Environ. 250 (2019) 429–439, https://doi.org/10.1016/j.apcatb.2019.01.065.

[18] K. Wetchakun, N. Wetchakun, S. Sakulsermsuk, An overview of solar/visible light-driven heterogeneous photocatalysis for water purification: TiO2- and ZnO-based photocatalysts used in suspension photoreactors, J. Ind. Eng. Chem. 71 (2019) 19–49, https://doi.org/10.1016/j.jiec.2018.11.025.

[19] A.M. Abdullah, M. Gracia-Pinilla, S.C. Pillai, K. O'Shea, UV and visible light-driven production of hydroxyl radicals by reduced forms of N, F, and P codoped titanium dioxide, Molecules 24 (2019) 2147, https://doi.org/10.3390/molecules24112147.

[20] S. Nagarajan, N.C. Skillen, F. Fina, G. Zhang, C. Randorn, L.A. Lawton, J.T. S. Irvine, P.K.J. Robertson, Comparative assessment of visible light and UV active photocatalysts by hydroxyl radical quantification, J. Photochem. Photobiol. A Chem. 334 (2017) 13–19, https://doi.org/10.1016/j.jphotochem.2016.10.034.

[21] I.K. Konstantinou, T.A. Albanis, Photocatalytic transformation of pesticides in aqueous titanium dioxide suspensions using artificial and solar light: Intermediates and degradation pathways, Appl. Catal. B Environ. 42 (2003) 319–335, https://doi.org/10.1016/S0926-3373(02)00266-7.

[22] J. Schneider, M. Matsuoka, M. Takeuchi, J Zhang, Y. Horiuchi, M. Anpo, D. W. Bahnemann, Understanding TiO2 photocatalysis: mechanisms and materials, Chem. Rev. 114 (2014) 9919–9986, https://doi.org/10.1021/cr5001892.

[23] A. Kafizas, X. Wang, S.R. Pendlebury, P. Barnes, M. Ling, C. Sotelo-Vazquez, R. Quesada-Cabrera, C. Li, I.P. Parkin, J.R. Durrant, Where do photogenerated holes go in anatase: rutile TiO2? A transient absorption spectroscopy study of charge transfer and lifetime, J. Phys. Chem. A. 120 (2016) 715–723, https://doi.org/10.1021/acs.jpca.5b11567.

[24] Y. Cai, Y.P. Feng, Review on charge transfer and chemical activity of TiO2: mechanism and applications, Prog. Surf. Sci. 91 (2016) 183–202, https://doi.org/10.1016/j.progsurf.2016.11.001.

[25] S.N. Ahmed, W. Haider, Heterogeneous photocatalysis and its potential applications in water and wastewater treatment: a review, Nanotechnology 29 (2018), 342001, https://doi.org/10.1088/1361-6528/aac6ea.

[26] Z. Shayegan, C.S. Lee, F. Haghighat, TiO2 photocatalyst for removal of volatile organic compounds in gas phase – a review, Chem. Eng. J. 334 (2018) 2408–2439, https://doi.org/10.1016/j.cej.2017.09.153.

[27] U.G. Akpan, B.H. Hameed, Parameters affecting the photocatalytic degradation of dyes using TiO2-based photocatalysts: a review, J. Hazard. Mater. 170 (2009) 520–529, https://doi.org/10.1016/j.jhazmat.2009.05.039.

[28] D. Friedmann, C. Mendive, D. Bahnemann, TiO2 for water treatment: Parameters affecting the kinetics and mechanisms of photocatalysis, Appl. Catal. B Environ. 99 (2010) 398–406, https://doi.org/10.1016/j.apcatb.2010.05.014.

[29] H. Gao, D. Zhang, M. Yang, S. Dong, Photocatalytic behavior of fluorinated rutile TiO2(110) surface: understanding from the band model, Sol. Rrl. 1 (2017), 1700183, https://doi.org/10.1002/solr.201700183.

[30] C. Minero, G. Mariella, V. Maurino, E. Pelizzetti, Photocatalytic transformation of organic compounds in the presence of inorganic anions. Hydroxyl-mediated and direct electron-transfer reactions of phenol on a titanium dioxide -fluoride system, Langmuir 16 (2000) 2632–2641, https://doi.org/10.1021/la9903301.

[31] Y. Xu, K. Lv, Z. Xiong, W. Leng, W. Du, D. Liu, X. Xue, Rate enhancement and rate inhibition of phenol degradation over irradiated anatase and rutile TiO2 on the addition of NaF: New insight into the mechanism, J. Phys. Chem. C. 111 (2007) 19024–19032, https://doi.org/10.1021/jp076364w.

[32] J. Ryu, W. Kim, J. Kim, J. Ju, J. Kim, Is surface fluorination of TiO2 effective for water purification? The degradation vs. mineralization of phenolic pollutants, Catal. Today 282 (2017) 24–30, https://doi.org/10.1016/j.cattod.2016.03.010.

[33] H. Park, Y. Park, W. Kim, W. Choi, Surface modification of TiO2 photocatalyst for environmental applications, J. Photochem. Photobiol. C. Photochem. Rev. 15 (2013) 1–20, https://doi.org/10.1016/j.jphotochemrev.2012.10.001.

[34] K. Lv, C.S. Lu, Different effects of fluoride surface modification on the photocatalytic oxidation of phenol in anatase and rutile TiO2 suspensions, Chem. Eng. Technol. 31 (2008) 1272–1276, https://doi.org/10.1002/ceat.200800041.

[35] N. Fessi, M.F. Nsib, L. Cardenas, C. Guillard, F. Dappozze, A. Houas, F. Parrino, L. Palmisano, G. Ledoux, D. Amans, Y. Chevalier, Surface and electronic features of fluorinated TiO2 and their influence on the photocatalytic degradation of 1-methylnaphthalene, J. Phys. Chem. C. 124 (2020) 11456–11468, https://doi.org/10.1021/acs.jpcc.0c01929.

[36] M. Mrowetz, E. Selli, H2O2 evolution during the photocatalytic degradation of organic molecules on fluorinated TiO2, N. J. Chem. 30 (2006) 108–114, https://doi.org/10.1039/b511320b.

[37] J.J. Murcia, M.C. Hidalgo, J.A. Navío, J. Araña, J.M. Doña-Rodríguez, Study of the phenol photocatalytic degradation over TiO2 modified by sulfation, fluorination, and platinum nanoparticles photodeposition, Appl. Catal. B Environ. 179 (2015) 305–312, https://doi.org/10.1016/j.apcatb.2015.05.040.

[38] S.Y. Yang, Y.Y. Chen, J.G. Zheng, Y.J. Cui, Enhanced photocatalytic activity of TiO2 by surface fluorination in degradation of organic cationic compound, J. Environ. Sci. 19 (2007) 86–89, https://doi.org/10.1016/S1001-0742(07)60014-X.

[39] H. Park, W. Choi, Effects of TiO2 surface fluorination on photocatalytic reactions and photoelectrochemical behaviors, J. Phys. Chem. B. 108 (2004) 4086–4093, https://doi.org/10.1021/jp036735i.

[40] Q. Wang, C. Chen, D. Zhao, M. Wanhong, J. Zhao, Change of adsorption modes of dyes on fluorinated TiO2 and its effect on photocatalytic degradation of dyes under visible irradiation, Langmuir 24 (2008) 7338–7345, https://doi.org/10.1021/la800313s.

[41] N. Jallouli, L.M. Pastrana-Martínez, A.R. Ribeiro, N.F.F. Moreira, J.L. Faria, O. Hentati, A.M.T. Silva, M. Ksibi, Heterogeneous photocatalytic degradation of ibuprofen in ultrapure water, municipal and pharmaceutical industry wastewaters using a TiO2/UV-LED system, Chem. Eng. J. 334 (2018) 976–984, https://doi.org/10.1016/j.cej.2017.10.045.

[42] M. Bosio, S. Satyro, J.P. Bassin, E. Saggioro, M. Dezotti, Removal of pharmaceutically active compounds from synthetic and real aqueous mixtures and simultaneous disinfection by supported TiO2/UV-A, H2O2/UV-A, and TiO2/

[43] H2O2/UV-A processes, Environ. Sci. Pollut. Res. 26 (2019) 4288–4299, https://doi.org/10.1007/s11356-018-2108-x.

[43] S. Romero, A. Villagomez, D. Trasviña, J. García, R. Gallegos, J. Reyes, J. Ramírez, F. Solís, Treatment and use of wastewater in Mexicali, Baja California, Mexico, WIT Trans. Ecol. Environ. 181 (2014) 591–602, https://doi.org/10.2495/EID140501.

[44] X. Van Doorslaer, J. Dewulf, J. De Maerschalk, H. Van Langenhove, K. Demeestere, Heterogeneous photocatalysis of moxifloxacin in hospital effluent: Effect of selected matrix constituents, Chem. Eng. J. 261 (2015) 9–16, https://doi.org/10.1016/j.cej.2014.06.079.

[45] J. Farner Budarz, A. Turolla, A.F. Piasecki, J.Y. Bottero, M. Antonelli, M. R. Wiesner, Influence of aqueous inorganic anions on the reactivity of nanoparticles in TiO2 photocatalysis, Langmuir 33 (2017) 2770–2779, https://doi.org/10.1021/acs.langmuir.6b04116.

[46] Z. Ran, L. Wang, Y. Fang, C. Ma, S. Li, Photocatalytic degradation of atenolol by TiO2 irradiated with an ultraviolet light emitting diode: Performance, kinetics, and mechanism insights, Catalysts 9 (2019) 876, https://doi.org/10.3390/catal9110876.

[47] T. Liu, K. Yin, C. Liu, J. Luo, J. Crittenden, W. Zhang, S. Luo, Q. He, Y. Deng, H. Liu, D. Zhang, The role of reactive oxygen species and carbonate radical in oxcarbazepine degradation via UV, UV/H2O2: Kinetics, mechanisms and toxicity evaluation, Water Res 147 (2018) 204–213, https://doi.org/10.1016/j.watres.2018.10.007.

[48] R.M. Castellanos, J. Paulo Bassin, M. Dezotti, R.A.R. Boaventura, V.J.P. Vilar, Tube-in-tube membrane reactor for heterogeneous TiO2 photocatalysis with radial addition of H2O2, Chem. Eng. J. 395 (2020), 124998, https://doi.org/10.1016/j.cej.2020.124998.

[49] J.C. Espíndola, R.O. Cristóvão, S.R.F. Araújo, T. Neuparth, M.M. Santos, R. Montes, J.B. Quintana, R. Rodil, R.A.R. Boaventura, V.J.P. Vilar, An innovative photoreactor, FluHelik, to promote UVC/H2O2 photochemical reactions: tertiary treatment of an urban wastewater, Sci. Total Environ. 667 (2019) 197–207, https://doi.org/10.1016/j.scitotenv.2019.02.335.

[50] A. Cabrera-Reina, A.B. Martínez-Piernas, Y. Bertakis, N.P. Xekoukoulotakis, A. Agüera, J.A.Sánchez Pérez, TiO2 photocatalysis under natural solar radiation for the degradation of the carbapenem antibiotics imipenem and meropenem in aqueous solutions at pilot plant scale, Water Res 166 (2019), 115037, https://doi.org/10.1016/j.watres.2019.115037.

[51] D. Lalliansanga, S.M. Tiwari, D.J. Lee, Kim, New insights in photocatalytic removal of alizarin yellow using reduced Ce3+/TiO2 catalyst, Environ. Sci. Pollut. Res (2020), https://doi.org/10.1007/s11356-020-11087-2.

[52] C.G. Hatchard, C.A. Parker, A new sensitive chemical actinometer - II. Potassium ferrioxalate as a standard chemical actinometer, Proc. R. Soc. London. Ser. A. Math. Phys. Sci. 235 (1956) 518–536. https://doi.org/10.1098/rspa.1956.0102.

[53] Y. Nosaka, A.Y. Nosaka, Generation and Detection of Reactive Oxygen Species in Photocatalysis, Chem. Rev. 117 (2017) 11302–11336, https://doi.org/10.1021/acs.chemrev.7b00161.

[54] Z.B. Alfassi, Peroxyl radicals in aqueous solutions. the Chemistry of free radicals: Peroxyl Radicals, 1st ed.,, Wiley-Blackwell Publishing Ltd,, New Jersey, 1997.

[55] C. Berberidou, V. Kitsiou, D.A. Lambropoulou, D. Michailidou, A. Kouras, I. Poulios, Decomposition and detoxification of the insecticide thiacloprid by TiO2-mediated photocatalysis: kinetics, intermediate products and transformation pathways, J. Chem. Technol. Biotechnol. 94 (2019) 2475–2486, https://doi.org/10.1002/jctb.6034.

[56] M. Muneer, D. Bahnemann, Semiconductor-mediated photocatalyzed degradation of two selected pesticide derivatives, terbacil and 2,4,5-tribromoimidazole, in aqueous suspension, Appl. Catal. B Environ. 36 (2002) 95–111, https://doi.org/10.1016/S0926-3373(01)00282-X.

[57] V. Augugliaro, M. Bellardita, V. Loddo, G. Palmisano, L. Palmisano, S. Yurdakal, Overview on oxidation mechanisms of organic compounds by TiO2 in heterogeneous photocatalysis, J. Photochem. Photobiol. C. Photochem. Rev. 13 (2012) 224–245, https://doi.org/10.1016/j.jphotochemrev.2012.04.003.

[58] C. Di Valentin, D. Fittipaldi, Hole scavenging by organic adsorbates on the TiO2 surface: A DFT model study, J. Phys. Chem. Lett. 4 (2013) 1901–1906, https://doi.org/10.1021/jz400624w.

[59] V.N. Despotović, B.F. Abramović, D.V. Šojić, S.J. Kler, M.B. Dalmacija, L.J. Bjelica, D.Z. Orčić, Photocatalytic degradation of herbicide quinmerac in various types of natural water, Water Air. Soil Pollut. 223 (2012) 3009–3020, https://doi.org/10.1007/s11270-012-1084-x.

[60] C.L. Greenstock, G.W. Ruddock, Determination of superoxide (O2-) radical anion reaction rates using pulse radiolysis, Pergamon Press,, 1976, https://doi.org/10.1016/0020-7055(76)90082-6.

[61] R.A. Palominos, M.A. Mondaca, A. Giraldo, G. Peñuela, M. Pérez-Moya, H. D. Mansilla, Photocatalytic oxidation of the antibiotic tetracycline on TiO2 and ZnO suspensions, Catal. Today 144 (2009) 100–105, https://doi.org/10.1016/j.cattod.2008.12.031.

[62] M. Pelaez, P. Falaras, V. Likodimos, K. O'Shea, A.A. de la Cruz, P.S.M. Dunlop, J. A. Byrne, D.D. Dionysiou, Use of selected scavengers for the determination of NF-TiO2 reactive oxygen species during the degradation of microcystin-LR under visible light irradiation, J. Mol. Catal. A Chem. 425 (2016) 183–189, https://doi.org/10.1016/j.molcata.2016.09.035.

[63] P.A. Babay, C.A. Emilio, R.E. Ferreyra, E.A. Gautier, R.T. Gettar, M.I. Litter, Kinetics and mechanisms of EDTA photocatalytic degradation with TiO2, 2001. https://doi.org/10.2166/wst.2001.0281.

[64] J. Theurich, M. Lindner, D.W. Bahnemann, Photocatalytic degradation of 4-chlorophenol in aerated aqueous titanium dioxide suspensions: a kinetic and mechanistic study, Langmuir 12 (1996) 6368–6376, https://doi.org/10.1021/la960228t.

[65] N. Watanabe, S. Horikoshi, H. Hidaka, N. Serpone, On the recalcitrant nature of the triazinic ring species, cyanuric acid, to degradation in Fenton solutions and in UV-illuminated TiO2 (naked) and fluorinated TiO2 aqueous dispersions, J. Photochem. Photobiol. A Chem. 174 (2005) 229–238, https://doi.org/10.1016/j.jphotochem.2005.03.013.

[66] G. Rózsa, Á. Fazekas, M. Náfrádi, T. Alapi, K. Schrantz, E. Takács, L. Wojnárovits, A. Fath, T. Oppenländer, Transformation of atrazine by photolysis and radiolysis: kinetic parameters, intermediates and economic consideration, Environ. Sci. Pollut. Res. 26 (2019) 23268–23278, https://doi.org/10.1007/s11356-019-05599-9.

[67] B.H.J. Bielski, D.E. Cabelli, R.L. Arudi, A.B. Ross, Reactivity of HO2/O2– radicals in aqueous solution, J. Phys. Chem. Ref. Data. 14 (1985) 1041–1100, https://doi.org/10.1063/1.555739.

[68] J.F. Montoya, P. Salvador, The influence of surface fluorination in the photocatalytic behaviour of TiO2 aqueous dispersions: an analysis in the light of the direct-indirect kinetic model, Appl. Catal. B Environ. 94 (2010) 97–107, https://doi.org/10.1016/j.apcatb.2009.10.025.

[69] M.S. Vohra, S. Kim, W. Choi, Effects of surface fluorination of TiO2 on the photocatalytic degradation of tetramethylammonium, J. Photochem. Photobiol. A Chem. 160 (2003) 55–60, https://doi.org/10.1016/S1010-6030(03)00221-1.

[70] S. Malato, J. Caceres, A. Agüera, M. Mezcua, D. Hernando, J. Vial, A.R. Fernández-Alba, Degradation of imidacloprid in water by photo-fenton and TiO2 photocatalysis at a solar pilot plant: A comparative study, Environ. Sci. Technol. 35 (2001) 4359–4366, https://doi.org/10.1021/es000289k.

[71] V. Kitsiou, N. Filippidis, D. Mantzavinos, I. Poulios, Heterogeneous and homogeneous photocatalytic degradation of the insecticide imidacloprid in aqueous solutions, Appl. Catal. B Environ. 86 (2009) 27–35, https://doi.org/10.1016/j.apcatb.2008.07.018.

[72] G. Sági, A. Bezsenyi, K. Kovács, S. Klátyik, B. Darvas, A. Székács, L. Wojnárovits, E. Takács, The impact of H2O2 and the role of mineralization in biodegradation or ecotoxicity assessment of advanced oxidation processes, Radiat. Phys. Chem. 144 (2018) 361–366, https://doi.org/10.1016/j.radphyschem.2017.09.023.

[73] S.L. Vinge, S.W. Shaheen, C.M. Sharpless, K.G. Linden, Nitrate with benefits: Optimizing radical production during UV water treatment, Environ. Sci. Water Res. Technol. 6 (2020) 1163–1175, https://doi.org/10.1039/c9ew01138b.

[74] L.F.B.A. Da Silva, N.M.M. Pires, T. Dong, H.C. Teien, Y. Yang, T. Storebakken, B. Salbu, The Role of Temperature, Ammonia and Nitrite to bioluminescence of Aliivibrio fischeri: Towards a new sensor for aquaculture, Proc. Annu. Int. Conf. IEEE Eng. Med. Biol. Soc. EMBS. 2018-July (2018) 4209–4212. ⟨https://doi.org/10.1109/EMBC.2018.8513283⟩.

[75] T. Løgager, K. Sehested, Formation and decay of peroxynitric acid: a pulse radiolysis study, J. Phys. Chem. 97 (1993) 10047–10052, https://doi.org/10.1021/j100141a025.

[76] A. Grigor'ev, I. Makarov, A. Pikaev, Formation of Cl2- in the bulk solution during the radiolysis of concentrated aqueous solutions of chlorides, High. Energy Chem. (Engl. Transl.); (U. S.) 21 (2) (1987) 99–102.

[77] S. Khan, X. He, J.A. Khan, H.M. Khan, D.L. Boccelli, D.D. Dionysiou, Kinetics and mechanism of sulfate radical- and hydroxyl radical-induced degradation of highly chlorinated pesticide lindane in UV/peroxymonosulfate system, Chem. Eng. J. 318 (2017) 135–142, https://doi.org/10.1016/j.cej.2016.05.150.

[78] G.V. Buxton, C.L. Greenstock, W.P. Helman, A.B. Ross, Critical Review of rate constants for reactions of hydrated electrons, hydrogen atoms and hydroxyl radicals (·OH/·O– in Aqueous Solution, J. Phys. Chem. Ref. Data. 17 (1988) 513–886, https://doi.org/10.1063/1.555805.

[79] S.G. Patra, A. Mizrahi, D. Meyerstein, The role of carbonate in catalytic oxidations, Acc. Chem. Res. 53 (2020) 2189–2200, https://doi.org/10.1021/acs.accounts.0c00344.

[80] O.N.E.H. Kaabeche, R. Zouaghi, S. Boukhedoua, S. Bendjabeur, T. Sehili, A comparative study on photocatalytic degradation of pyridinium-based ionic liquid by TiO2 and ZnO in aqueous solution, Int. J. Chem. React. Eng. 17 (2019) 1–14, https://doi.org/10.1515/ijcre-2018-0253.

[81] M.L. Dell'Arciprete, J.M. Soler, L. Santos-Juanes, A. Arques, D.O. Mártire, J.P. Furlong, M.C. Gonzalez, Reactivity of neonicotinoid insecticides with carbonate radicals, Water Res 46 (2012) 3479–3489, https://doi.org/10.1016/j.watres.2012.03.051.